2026 IEEE/SICE International Symposium on System Integration (SII)
January 11-14, 2026. Cancún, México

Development of a Gel Urethra Model Simulator Using Agarose-PEG and Performance Evaluation of a Soft Growing Actuator for Urinary Catheter Insertion Assistance

K. Kishino, *Student Member, IEEE,* R. Sasaki, F. Ito, *Member, IEEE,*
H. Yamanaka, M. Komeya, and T. Nakamura, *Member, IEEE*

Abstract— **This paper proposes a urinary catheter insertion assistance mechanism aimed at reducing pain and the risk of injury during insertion, as well as an agarose–PEG gel urethra model simulator for its performance evaluation. Conventional urinary catheterization has the drawback that friction against the urethral wall and impingement at curved sections can cause severe pain and tissue damage to patients. To address this, we focused on a soft growing actuator that can advance through a lumen without sliding its outer surface, and we developed a urinary catheter insertion assistance mechanism utilizing this actuator. In addition, we newly developed a gel-based urethra model simulator, made of agarose and PEG, capable of reproducing urethral length, diameter, curvature geometry, and Young's modulus, and used it for performance evaluation of the proposed mechanism. Fundamental property tests confirmed that gel containing 2% agarose and 20% PEG achieved a Young's modulus (~125 kPa) equivalent to that of the urethra and exhibited high toughness. In insertion experiments using the urethra model simulator, the proposed mechanism demonstrated stable extension and catheter traction even in models with curvature or straight-section stenosis. These results indicate that a urinary catheter insertion assistance mechanism employing a soft growing actuator has the potential to effectively reduce friction and alleviate pain inside the urethra.**

I. Introduction

A urinary catheter is a flexible tube used to drain urine from the bladder to the outside in patients who have difficulty urinating independently, and it is widely used in clinical settings including urology and perioperative care [1–2]. In cases where urinary retention occurs due to benign prostatic hyperplasia or urethral stricture, as well as neurogenic bladder caused by aging, spinal cord injury, advanced dementia, or multiple sclerosis, the use of a urinary catheter becomes indispensable [3–5]. Urinary catheters are also used for bladder management before and after surgery and for intravesical drug administration. Persistent urinary retention can cause complications such as deterioration of renal function, urinary tract infection, bladder stones, and urinary leakage, so proper urination management is required [3]. Urinary catheters are classified into two types: intermittent catheters, which are removed after urination, and indwelling catheters, which can be fixed in the bladder by a balloon for long-term placement. The latter is widely used for long-term management due to the convenience of not requiring repeated insertion [4].

On the other hand, the use of urinary catheters imposes various burdens on patients. Typical complications include urinary tract infection, damage to the urethra, prostate, and bladder, scarring and urethral stricture, bladder muscle spasms, as well as bleeding and urinary leakage [3]. Particularly, when inserting a catheter for the first time or replacing it, severe pain often occurs during the process of advancing the catheter from the urethral meatus to the bladder. The main causes are friction with the urethral wall and tissue damage caused by the catheter tip striking the curved portions of the urethra. To address such pain and discomfort, lubricants, anesthetic gels, warming of the catheter, and appropriate size selection have conventionally been used [4–5], but these measures do not fundamentally reduce the physical invasion of the urethra itself. Therefore, in the narrow lumen of the urethra (minimum diameter 6 mm), a new catheter insertion method that can suppress friction and impingement and reduce patient pain and the risk of complications is expected.

In previous research, several assistive devices have been developed to address difficult urinary catheter insertions or to reduce patient burden. For example, the Urethral Catheterisation Device (UCD®) [6] by Urethrotech is an indwelling catheter integrated with a hydrophilic guidewire, and has been reported to enable smooth and safe catheter advancement in cases where insertion is difficult, such as with prostatic hypertrophy or urethral stricture. Attempts have also been made to automate catheter insertion, with prototypes of automated insertion devices incorporating lubrication and insertion force control using a stepper motor being reported [7]. These devices have shown usefulness in terms of standardizing techniques, reducing operator dependence, and addressing difficult cases. However, their main purpose is to assist catheter advancement, and they do not reduce damage such as friction with the urethral wall or impingement at curved portions.

In this study, we develop a urinary catheter insertion assistance mechanism to reduce patient burden. We focus on the soft growing actuator [8–10], a mechanism inspired by plant growth movements that allows advancement into fragile and narrow environments such as disaster sites. This actuator is a flexible advancement mechanism using a thin-walled tube. One end is fixed to a pressurization device, the other end is sealed and folded inward. When air pressure is applied inside, the folded portion everts outward and extends forward.

K. Kishino, R. Sasaki, F. Ito and T. Nakamura are with the Department of Precision Mechanics, Faculty of Science and Engineering, Chuo University, 1-13-27 Kasuga, Bunkyo-Ku, Tokyo, 112-8551, Japan (corresponding author to provide e-mail: k_kishino@bio.mech.chuo-u.ac.jp).

H. Yamanaka and M. Komeya are with the Department of Urology, Faculty of Medicine, Yokohama City University, 3-9 Hukuura, Kanazawa-Ku, Yokohama 236-0004, Japan (e-mail: komeyam@yokohama-cu.ac.jp).

978-1-6654-5784-2/26/$31.00 ©2026 IEEE

Because the outer surface does not slide against the environment, friction inside the lumen is reduced and the risk of damage can be minimized. In previous studies, most soft growing actuators were relatively large, with an inner diameter of about 25 mm, but miniaturization to about 2.3 mm has recently been achieved, and applications in the medical field such as bronchial navigation are being explored [8,11,12]. We hypothesized that placing a urinary catheter inside this actuator and pulling it could allow it to advance into the bladder while suppressing friction and collisions at curved portions inside the urethra.

In prior research [13], a small 6.0 mm diameter soft growing actuator was prototyped using a low-density polyethylene (LDPE) sheet with a thickness of 0.06 mm and low friction. By forming and heat-welding this sheet, extension inside an S-shaped tube model was achieved, pulling a 3.0 mm diameter wire to the bladder position. However, the model used was a simple rubber tube with an outer diameter of 12.0 mm, and did not sufficiently reproduce the shape, inner diameter, or hardness of the urethra. In addition, the traction target was limited to a wire, without verification for catheter traction, and no evaluation of damage to the urethral wall was performed, making clinical application difficult. Models simulating biological lumens have been developed for various purposes such as medical education and device performance evaluation. Representative examples include vascular and bronchial models made from silicone or polyurethane [14,15]. While these have excellent moldability and durability and can be reused, their elastic modulus and friction properties differ significantly from actual tissues, limiting their ability to reproduce deformation and contact behavior specific to soft tissue. Existing models for the urethra include silicone male urethra models for education, but they do not sufficiently reproduce clinically important features such as changes in inner diameter by region, curved shapes, hardness distribution, and stenotic lesions.

Therefore, this paper reports on a newly developed urinary catheter insertion assistance mechanism using a soft growing actuator, and a gel-based urethra model simulator that simulates urethral characteristics. The aim was to enable insertion tests in a conduit close to the urethra and to evaluate the performance and effectiveness of the proposed mechanism.

In the following, Section II describes the insertion assistance mechanism and soft growing actuator, Sections III and IV describe the fabrication method and fundamental property tests of the urethra model simulator, Section V reports operational experiments in the gel model, and Section VI presents conclusions and future perspectives.

II. Mechanism

In this study, we propose a urinary catheter insertion assistance mechanism as shown in Fig. 1(a). This mechanism consists of a compressor, a pressure regulator, a pressurization chamber, a soft growing actuator, a urinary catheter, and a urethra model simulator. In this section, the outline of the proposed urinary catheter insertion assistance mechanism, as well as the principle and fabrication method of the soft growing actuator, are described.

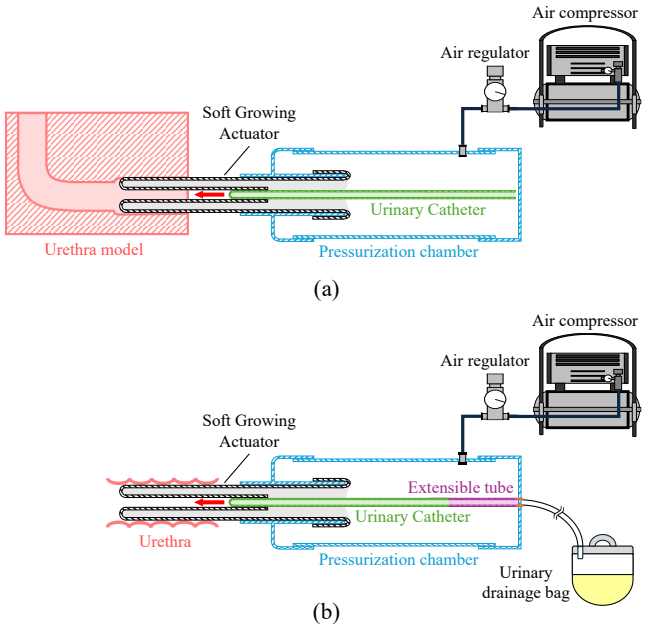

Figure 1. (a) Overview of the proposed mechanism. (b) Future concept with urinary drainage function in the proposed mechanism.

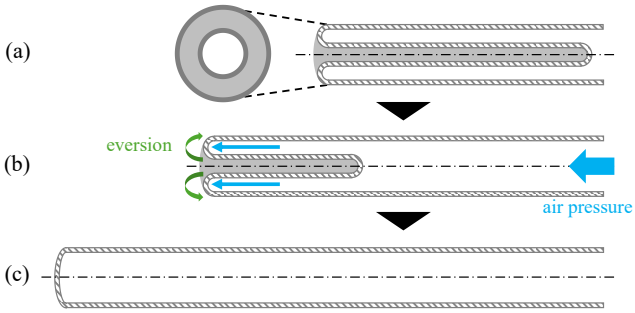

Figure 2. Cross sectional view of the thin-walled tubular soft growing actuator. (a) Before (b) During (c) After application of air pressure.

A. Urinary Catheter Insertion Assistance Mechanism

An overview of the proposed mechanism is shown in Fig. 1(a). Air from the compressor is supplied to the soft growing actuator via a pressure regulator and a pressurization chamber. As the soft growing actuator extends under air pressure, the urinary catheter connected to its tip is pulled into the urethra model simulator. In future applications, as shown in Fig. 1(b), it is envisioned that an extensible tube and a urine drainage bag will be connected to the distal end of the urinary catheter, and urination will be promoted via the pressurization chamber.

B. Soft Growing Actuator

The operating principle of the soft growing actuator is shown in Fig. 2. The actuator operates according to the sequence illustrated in Figs. 2(a)–(c). (a) One end of the actuator is heat-sealed to prevent air leakage, and the tube is folded inward. The length of the folded portion corresponds to

the maximum extendable length of the actuator. The other end is fixed to the pressurization device in an airtight manner. (b) Air pressure is applied inside the folded actuator from the pressurization device, pushing the folded section at the actuator tip forward. (c) The inner tube inverts outward, extending the actuator forward without sliding its outer surface against the surrounding environment. By executing these steps from (a) to (c), the soft growing actuator operates.

Table I lists the required specifications for the soft growing actuator, taking into account its operating principle and intended use in the male urethra. Based on these specifications, the actuator was fabricated using the process shown in Fig. 3(a). A polyethylene (PE) sheet with a thickness of 0.06 mm and an aluminum pipe were prepared. The PE sheet was wrapped around an aluminum pipe of 6.0 mm outer diameter with an overlap of about 5 mm. One overlapped edge was temporarily heat-sealed with a spatula-type sealer to form a tube shape. Finally, the tubular PE sheet was passed through a plastic plate (7.0 mm wide, 0.7 mm thick), and the overlapped portion was re-sealed with a sealer to prevent air leakage from the weld. The fabricated soft growing actuator is shown in Fig. 3(b).

TABLE I REQUIREMENTS OF SOFT GROWING ACTUATOR

Requirement	***Specification***	***Rationale***
Material property	Invertible material	To enable inversion under pneumatic pressure
Surface property	Smooth extension with minimal friction	To enable smooth extension and prevent damage to urethral wall
Airtightness	No air leakage	To ensure stable pneumatic actuation
Outer diameter	6 mm	To fit within male urethral diameter (6–15 mm)
Extendable length	200–230 mm	To fit within male urethral length (180–200 mm)

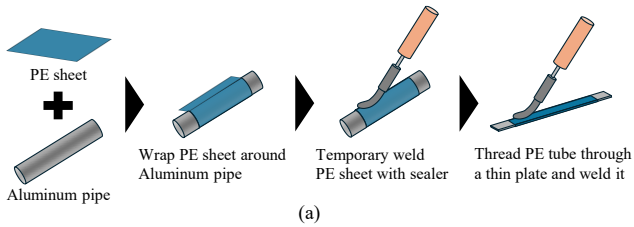

(a)

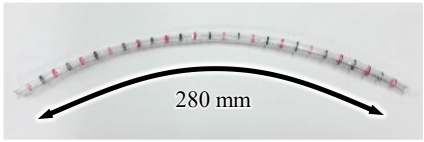

(b)

Figure 3. (a) Fabrication method of soft growing actuator. (b) Soft growing actuator.

III. URETHRA MODEL SIMULATOR

In this study, we fabricated a urethra model simulator that reproduces the measured length, diameter, curvature angle, and radius of curvature of the urethra. Because this model is gel-based, it can reproduce stenosis in both straight and curved sections. By combining agarose and polyethylene glycol 400 (PEG), the model can replicate the Young's modulus of the urethra in its initial strain region, thereby providing a flexibility not found in conventional rigid models. This section describes the fabrication method of the gel urethra model simulator.

A. Structure and Mechanical Properties of the Urethra

The structure of the adult male urethra is shown in Fig. 4. A healthy adult male urethra is 180–200 mm in length and 6–15 mm in internal diameter [16,17]. The urethra passes through the prostatic urethra just below the bladder, then exhibits a bend of 90–120° near the membranous urethra and bulbous urethra [18]. It also bends again midway along the penile urethra, but during catheterization, the penis is generally lifted to straighten it. Urethral stricture occurs mainly in two locations: in the prostatic urethra near the bend in cases of urinary retention due to prostatic hypertrophy, and in the straight section such as the penile urethra in cases of scarring or trauma. Typical strictures have a diameter of about 3–5 mm and a length of 10–40 mm.

According to [19], stress relaxation tests on male cadaver urethra samples have been conducted to evaluate mechanical properties. The Young's modulus in the initial strain region in the longitudinal direction was reported to be 5.4 kPa for the membranous urethra, 130.0 kPa for the bulbous urethra, and 120.0 kPa for the penile urethra, reflecting the flexibility and deformation resistance of each part.

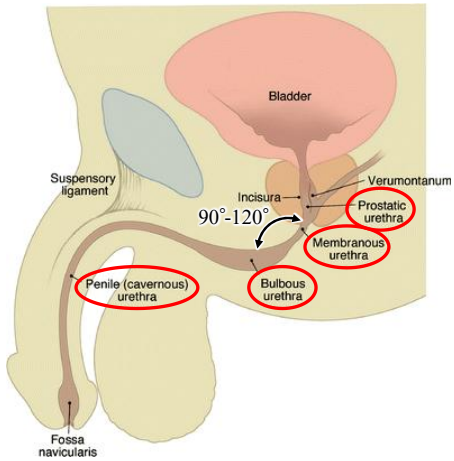

Figure 4. Anatomy of male urethra [17].

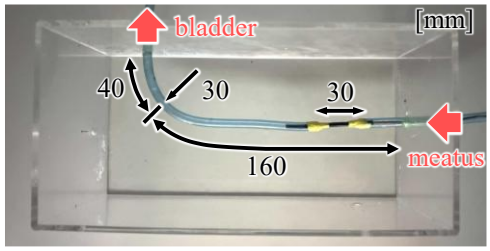

Figure 5. The mold of gel urethra model simulator.

B. Fabrication Method

Agarose gel at 1–2% concentration is widely used in tissue-mimicking models [20,21]. In this study, based on this knowledge and preliminary experiments confirming operation of the soft growing actuator in a straight 2% agarose model, the urethra model simulator was fabricated using 2% agarose as the base material. In addition, because agarose alone is brittle and prone to cracking, PEG — commonly used as a phantom material in medical applications — was added to reproduce the Young's modulus of the urethra. The target Young's modulus was set to 120–130 kPa, based on Section III-A, corresponding to that of the bulbous and penile urethra, which account for most of the urethral length.

The urethra model simulator was fabricated using the mold shown in Fig. 5 (90° bend, straight stenosis). Two holes were drilled in a rectangular plastic container, and a polyurethane tube with an outer diameter of 6.0 mm was passed along the urethral path. The bend was positioned 40 mm from the bladder side, with a radius of curvature of 3 mm and bend angles of either 90° or 120°. To create a stenosis, a section of 3 mm outer diameter tubing was inserted into the 6.0 mm tubing. The stenosis length was set to 30 mm and located either in the straight section (30–60 mm from the urethral meatus) or in the curved section (10–40 mm from the bladder). The fabrication procedure was as follows:

[1] Suspend agarose powder in water and completely dissolve it by heating in a microwave.

[2] Add an appropriate amount of PEG and stir to improve the toughness of the agarose.

[3] Pour the solution into the urethra model mold.

[4] After gelation, remove the polyurethane tube and demold.

In Section IV, compression tests of multiple samples with varying PEG concentrations were used to determine the optimal composition for the urethra model simulator.

IV. Fundamental Property Tests

In this section, we describe the fundamental property tests of the agarose–PEG gel performed for the fabrication of the urethra model simulator.

A. Purpose of the Experiment

Compression tests were conducted on gels with different PEG concentrations to determine the Young's modulus, to establish the PEG concentration suitable for the urethra model simulator. In addition, the effect of PEG concentration on the Young's modulus of the gel was examined.

B. Experimental Conditions

Cylindrical samples were compressed using a tensile/compression tester (AIKOH ENGINEERING, MODEL-1308U), and the force applied to the specimen and the displacement of the specimen were measured. Circular plates with a diameter of 40 mm and thickness of 10 mm were attached to the upper and lower compression parts of the testing machine, and cylindrical specimens with a diameter of 20 mm and a height of 20 mm were used. The following four compositions were tested: (i) 2% agarose only, (ii) 2% agarose + 15% PEG, (iii) 2% agarose + 20% PEG, (iv) 2% agarose + 25% PEG. Three specimens were prepared for each composition, and three compression trials were performed for each specimen. From the recorded force and displacement data, stress and strain were calculated, and stress–strain curves for each composition were obtained as the average of the three trials. Nominal stress and nominal strain were calculated without considering changes in specimen diameter due to compression. From these stress–strain curves, Young's modulus in the initial strain range (0–0.1) was determined and compared with the target value of 120–130 kPa.

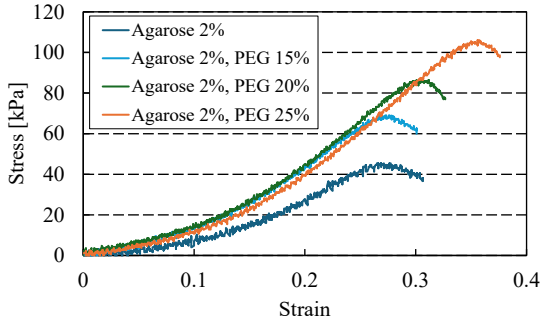

Figure 6. Stress-strain curves obtained by compression testing of each agarose-PEG gel.

TABLE II Mechanical Properties of Each Agarose-PEG Gel

	gel components	*Young's modulus* [kPa]	*fracture strength* [kPa]
(i)	agarose 2%	99.4	45.4
(ii)	agarose 2% PEG 15%	128.8	69.0
(iii)	agarose 2% PEG 20%	125.3	86.5
(iv)	agarose 2% PEG 25%	112.8	106.1

C. Results and Discussion

The stress–strain curves derived from the measured force and displacement are shown in Fig. 6. Table II shows the Young's modulus in the strain range 0–0.1 and the fracture strength for each condition. Condition (i), 2% agarose only, had a Young's modulus of 99.4 kPa, which was relatively low and somewhat brittle for mimicking the urethral wall. In contrast, adding PEG increased the Young's modulus: (ii) 15% PEG reached 128.8 kPa, and (iii) 20% PEG reached 125.3 kPa, both within the target range of 120–130 kPa. This is thought to be due to changes in the gel's internal network structure caused by PEG addition, increasing stiffness. However, (iv) 25% PEG showed a lower Young's modulus of 112.8 kPa, possibly due to excessive PEG addition disrupting the gel's hydration state and network structure, resulting in softening. This suggests that excessively high PEG concentrations may reduce the strength and stability of the gel. On the other hand, fracture strength increased with PEG concentration, reaching a maximum of 106.1 kPa at (iv) 25% PEG. Materials with high fracture strength are less likely to fail under deformation or impact and are considered capable of reproducing the toughness of biological tissue. From the above, (iii) 20% PEG

was judged to be optimal for the urethra model simulator, as it had a Young's modulus within the target range and high fracture strength with excellent toughness. In Section V, we perform catheter traction experiments using the soft growing actuator in the urethra model simulator fabricated with 2% agarose and 20% PEG.

V. Experiment in the Urethra Model Simulator

In this section, we describe the operation experiments in which the soft growing actuator was used to pull a urinary catheter through multiple types of urethra model simulators.

A. Purpose of the Experiment

The aim was to verify whether the soft growing actuator could extend and pull a urinary catheter in a gel-based urethra model simulator made of 2% agarose and 20% PEG, which reproduces the Young's modulus of the urethra. Furthermore, the effect of changing the curvature and stenosis conditions of the urethra model simulator on the extension of the soft growing actuator was examined.

B. Experimental Conditions

The appearance of the soft growing actuator and pressurization chamber is shown in Fig. 7, and the six types of urethra model simulators used are shown in Fig. 8. Air pressure was applied to the pressurization chamber to extend the soft growing actuator inside the urethra model simulator. The actuator used had a thickness of 0.06 mm, an inner diameter of 6 mm, a total length of 280 mm, and an extendable length of 200 mm. The applied pressure was 90 kPa. The conditions of the urethra model simulators were as follows: (i) 90° bend, no stenosis (ii) 90° bend, straight-section stenosis (iii) 90° bend, curved-section stenosis (iv) 120° bend, no stenosis (v) 120° bend, straight-section stenosis (vi) 120° bend, curved-section stenosis. The urethra model simulators had a total thickness of 36 mm, providing at least 15 mm of wall thickness around the 6 mm urethral lumen. The extension process was recorded with a camera, and the trajectory of the actuator's inversion tip was tracked using Kinovea (ver. 2023.1.2) to obtain graphs of extension distance versus time.

C. Results and Discussion

The extension of the soft growing actuator inside the urethra model simulator ((i) 90°, no stenosis) is shown in Fig. 9. The relationship between the extension distance of the actuator tip and time is shown in Fig. 10. For conditions with curved-section stenosis ((iii) and (vi)), penetration occurred during extension, so data for those conditions are excluded from the graph. Under conditions without stenosis ((i) 90°, no stenosis and (iv) 120°, no stenosis), steep extension occurred immediately after initiation, reaching the maximum extension (~200 mm) within 8 s for (i) and within 5 s for (iv). This is attributed to minimal frictional resistance with the lumen wall, as the actuator's outer surface did not slide significantly against the environment. For straight-section stenosis ((ii) 90° and (v) 120°), maximum extension (~200 mm) was also achieved, but a gradual progression was observed at an extension distance of about 50 mm. This corresponds to the actuator tip reaching the stenosis, where circumferentially distributed internal pressure gradually expanded the stenosis, temporarily reducing the extension speed. After passing through, resistance decreased, and steep extension resumed around 40–50 s. In these straight-section stenosis conditions, although extension succeeded, cracks were observed in the stenosis region (Fig. 11(a)). These cracks are thought to result from local tearing stress applied to the gel urethral wall by circumferential forces from the inversion surface while prying open the stenosis. For clinical application, limiting the maximum applied pressure, using lubricants to distribute stress, or employing pulsed pressurization at step changes may be effective in reducing the risk of damage. For curved-section stenosis ((iii) 90° and (vi) 120°), the actuator tip caught on the step at the curved stenosis, and penetration occurred due to local stress concentration (Fig. 11(b)). When curvature and stenosis overlap, the mechanical conditions may favor perforation rather than overcoming the step. Curved-section stenoses often form in conditions such as prostatic hypertrophy, where mechanical properties depend on the surrounding prostate or fibrotic tissue rather than the original urethral tissue. Future work should investigate existing literature and clinical findings on the stiffness and structure of stenotic tissue and re-verify inversion behavior using models incorporating these characteristics. Comparing 90° and 120° bends, in conditions without stenosis, 120° bends reached maximum extension faster, suggesting that gentler curvature is advantageous for inversion progression. Similarly, for straight-section stenosis, slight deceleration was observed at around 44–47 s for 90°, indicating that sharper bends (90°) increase the bending resistance of the inversion surface, making final progression relatively more difficult. Overall, this mechanism can extend relatively stably through bends and straight-section stenoses, but curved-section stenoses tend to cause penetration, and straight-section stenoses tend to cause cracks. Improvements such as pressure control and enhanced reproducibility of stenosis are necessary.

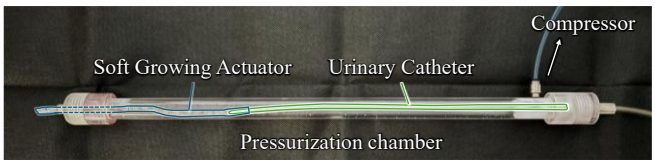

Figure 7. The appearance of the soft growing actuator and pressurization chamber.

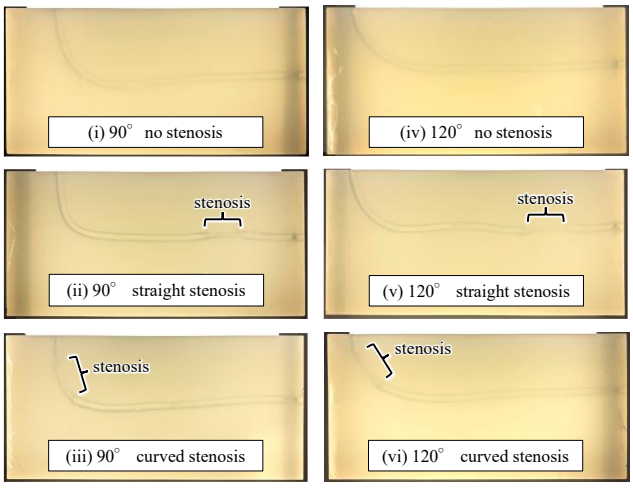

Figure 8. Gel urethra model (i)–(vi).

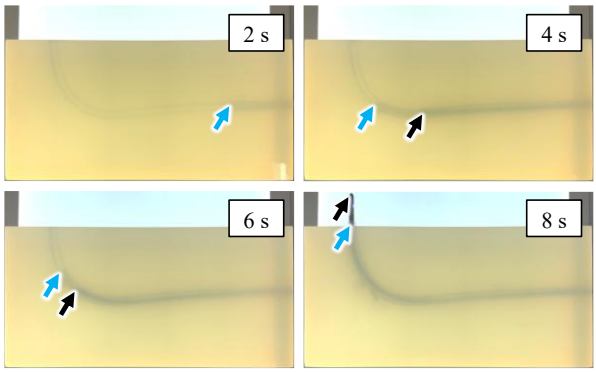

Figure 9. Extension of soft growing actuator in urethra model simulator (i) 90°, none stenosis. The blue arrow indicates the position of the tip of the soft growing actuator, and the black arrow indicates the position of the tip of the catheter.

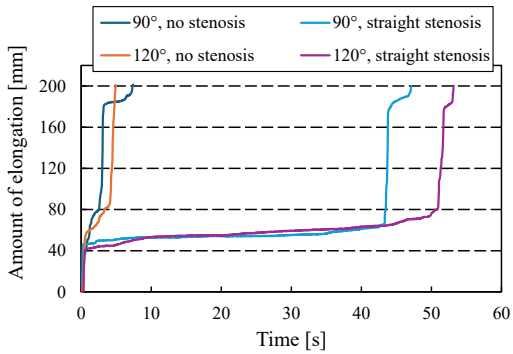

Figure 10. Elongation of soft growing actuator at each urethra model simulator.

(a) (b)

Figure 11. (a) Crack ((v) 120°, straight stenosis) and (b) penetration ((vi) 120°, curved stenosis) in the urethra model simulator.

VI. Conclusion

In this paper, we proposed a urethra model simulator made of agarose and PEG based on the mechanical properties of the urethra and reported an evaluation of damage during urinary catheter insertion using a soft growing actuator. Extension within a urethra model simulator having a Young's modulus equivalent to that of the urethra was achieved. In future work, we will first conduct multi-cycle experiments to verify the reproducibility of both the soft growing actuator and the urethra model simulator, since each condition was tested only once in this paper. Then, we plan to embed pressure sensors inside the urethra model simulator to quantify parameters such as insertion force, friction, and internal pressure. Using these quantitative data, we will then compare actuator-driven insertion with conventional manual catheter insertion to clarify the usefulness of the proposed insertion assistance mechanism.

Acknowledgment

This work was supported by the Sekisui Chemical Co., Ltd. "Inspiration from Nature" Research Grant Program and by AMED under Grant Number JP25hma322039.

References

[1] Y. Igawa et al., "Catheterization: Possible Complications and Their Prevention and Treatment." International Journal of Urology, vol. 15, no. 6, pp. 481–485, 2008.
[2] N. Marjanovic, C. Luciano and C. Niederberger, "CathSym: Device and Method to Bring Haptic Feedback to Urinary Catheterization Training," 2021 43rd Annual Int. Conf. of the IEEE Engineering in Medicine & Biology Society (EMBC), Mexico, pp. 4908-4911, 2021.
[3] Cleveland Clinic, "Urinary Catheter - Cleveland Clinic," https://my.clevelandclinic.org/health/treatments/catheter, (accessed Aug. 2025).
[4] NHS, "Urinary catheters," https://www.nhs.uk/tests-and-treatments/urinary-catheters/, (accessed Aug. 2025).
[5] National Library of Medicine, "Bladder Catheterization – StatPearls," https://www.ncbi.nlm.nih.gov/books/NBK560748/, (accessed Aug. 2025).
[6] Urethrotech, "Urethrotech: Urethral Catheterization Device," https://urethrotech.com/, (accessed Aug. 2025).
[7] S. Kang et al., "A feasibility study using cadaver: Efficacy and safety of the novel automatic urinary catheterization device," Medicine vol. 97, no. 51, 2018.
[8] T. Yanagida, K. Adachi and T. Nakamura, "Development of endoscopic device to veer out a latex tube with jamming by granular materials," 2013 IEEE Int. Conf. on Robotics and Biomimetics (ROBIO), Shenzhen, China, pp. 1474-1479, 2013.
[9] H. Tsukagoshi, N. Arai, I. Kiryu and A. Kitagawa, "Smooth creeping actuator by tip growth movement aiming for search and rescue operation," 2011 IEEE Int. Conf. on Robotics and Automation, Shanghai, China, pp. 1720-1725, 2011.
[10] E. W. Hawkes et al., "A soft robot that navigates its environment through growth," Sci. Robot. 2, eaan3028, 2017.
[11] C. Girerd et al., "Material Scrunching Enables Working Channels in Miniaturized Vine-Inspired Robots," in IEEE Transactions on Robotics, vol. 40, pp. 2166-2180, 2024.
[12] J. Davy et al., "Vine Robots With Magnetic Skin for Surgical Navigations," in IEEE Robotics and Automation Letters, vol. 9, no. 8, pp. 6888-6895, 2024.
[13] K. Kishino et al., "Development of a Soft Growing Actuator for Automated Cystoscope Insertion," IEEE/SICE International Symposium on System Integration (SII), Munich, Germany, 2025.
[14] Eva García-Carpintero et al., "Phantoms for ultrasound-guided vascular access cannulation training: a narrative review," Medical ultrasonography, vol. 25, no. 2, pp. 201-207, 2023.
[15] J. Ock et al., "Patient-specific and hyper-realistic phantom for an intubation simulator with a replaceable difficult airway of a toddler using 3D printing," Sci. Rep., vol. 10, 10631, 2020.
[16] C. Masri et al., "Experimental characterization and constitutive modeling of the biomechanical behavior of male human urethral tissues validated by histological observations," Biomechanics and modeling in mechanobiology, vol. 17, no. 4, pp. 939-950, 2018.
[17] T. L. Levin et al., "Congenital anomalies of the male urethra," Pediatric radiology, vol. 37, no. 9, pp. 851-862; 2007.
[18] IMIOS, "Membranous part of male urethra," https://www.imaios.com/en/e-anatomy/anatomical-structures/membranous-part-of-male-urethra-1541216156#, (accessed Aug. 2025).
[19] A. Berardo et al., "Mechanical Characterization of the Male Lower Urinary Tract: Comparison among Soft Tissues from the Same Human Case Study," Applied Sciences 14, no. 4: 1357, 2024.
[20] A. I. Chen et al., "Multilayered tissue mimicking skin and vessel phantoms with tunable mechanical, optical, and acoustic properties," Medical physics, vol. 43, no. 6, pp. 3117-3131, 2016.
[21] A. Tejo-Otero et al., "Soft-Tissue-Mimicking Using Hydrogels for the Development of Phantoms," Gels, vol. 8, no. 1, Basel, Switzerland, 2022.